$Tb_{0.67}PdAl_3$ and $Gd_{1.33}Pt_3Al_8$ with layers of rare-earth-metal atoms and Al-atom triangles

Yuriy LUTSYSHYN[1]*, Yaroslav TOKAYCHUK[1], Volodymyr DAVYDOV[1], Roman GLADYSHEVSKII[1]

[1] *Departement of Inorganic Chemistry, Ivan Franko National University of Lviv,*
Kyryla i Mefodiya St. 6, 79005 Lviv, Ukraine
* *Corresponding author. Tel.: +380-32-2394163; e-mail: lutsyshyn@ukr.net*

The crystal structures of the ternary compounds $Tb_{0.67}PdAl_3$ ($hP14$-4.67, $P6_3/mmc$, $a = 4.394(4)$, $c = 9.372(6)$ Å) and $Gd_{1.33}Pt_3Al_8$ ($hR51$-14.00, $R\bar{3}m$, $a = 4.3090(14)$, $c = 38.54(2)$ Å) were refined from X-ray single-crystal diffraction data. They contain monoatomic layers stacked along [001] with ordered or disordered distribution of rare-earth-metal atoms and Al-atom triangles. Together with the structures of $Y_2Co_3Ga_9$, $Sc_{0.67}Fe_2Si_5$, $Er_4Pt_9Al_{24}$, and $ErNi_3Al_9$, they form a family of intergrowth structures built up of three kinds of monoatomic layer. Analyzing the relative positions of the monoatomic layers, some basic stacking rules, which may help to predict new structures, are formulated.

Aluminide / Rare-earth metal / Noble metal / Single-crystal X-ray diffraction / Intergrowth layered structure

Introduction

The Al-rich parts of the phase diagrams of *R*-*T*-Al systems, where *R* is a rare-earth metal and *T* a *d*-element of group VIII, appear to be very complicated and a large number of ternary compounds containing >60 at.% Al have been reported [1]. Ternary aluminides crystallizing with 28 different structure types are listed in Table 1. Nine types among these, *i.e.* $ErNi_3Al_9$ [16], $DyNi_3Al_9$ [16], $Sc_{0.67}Fe_2Si_5$ [19], $Gd_{1.33}Pt_3Al_8$ [20], $Er_{1.33}Pt_3Al_8$ [21], $Er_4Pt_9Al_{24}$ [21], $Y_4Pt_9Al_{24}$ [21], $Y_2Co_3Ga_9$ [22], and $Ho_2Rh_3Al_9$ [23], are characterized by the presence of Al-atom triangles. These triangles and rare-earth-metal atoms are distributed in the ratio 1:2 in layers. Such compounds form in a rather narrow range of Al content (64.3-69.2 at.%) and their structures may be completely decomposed into monoatomic (one-atom thick) layers.

The aim of the persent work was to study this group of ternary aluminides containing ordered or disordered layers with *R* atoms and Al_3 triangles, formulate some basic stacking rules for the layers, and search for new representatives with rare-earth metals and *d*-elements of group VIII.

Experimental

Alloys were synthesized from the elements (Tb ≥ 99.83 wt.%, Gd ≥ 99.86 wt.%, Pd ≥ 99.9 wt.%, Pt ≥ 99.9 wt.%, Al 99.998 wt.%) by arc melting in a water-cooled copper crucible under a purified argon atmosphere, using Ti as a getter and a tungsten electrode. The ingots were annealed at 600ºC in quartz ampoules under vacuum for 1 month and subsequently quenched in cold water. The weight losses during the preparation of the samples were less than 0.5 % of the total mass, which was 1 g for each alloy.

Single crystals were extracted from alloys of nominal compositions $Tb_{11}Pd_{24}Al_{65}$ and $Gd_{14}Pt_{21}Al_{65}$ (in at.%). They were mounted on glass fibers and X-ray diffraction data were collected in the ω-2θ scan mode at room temperature on a CAD-4T diffractometer (Mo $K\alpha$ radiation, $\lambda = 0.71073$ Å). An analytical absorption correction was applied. No significant variation of the intensities was observed during the data collections. Cell parameters were obtained by a least-squares refinement of the angles of 25 reflections for each crystal. For the Tb-containing crystal, the systematic extinctions (*hhl* and 00*l*: $l = 2n+1$) indicated as possible space groups $P6_3mc$, $P\bar{6}2c$, and $P6_3/mmc$ [27]. The structure was solved by direct methods in the centrosymmetric space group $P6_3/mmc$, using the SHELXS-97 program [28], leading to the composition $Tb_{0.67}PdAl_3$. A full-matrix least-squares refinement of the positional and anisotropic displacement parameters was performed on F^2 using the SHELXL-97 program [28]. Trial refinements in the noncentrosymmetric space groups $P6_3mc$ and $P\bar{6}2c$ did not improve the results. In the case of the Gd-containing crystal, the atomic coordinates reported for $Gd_{1.33}Pt_3Al_8$ (space group

Table 1 Structure types of ternary aluminides of rare-earth metals and *d*-elements of group VIII containing >60 at.% Al [1].

At.% Al	Compound	Structure type	Pearson symbol	Space group	Ref.
76.9	RFe_2Al_{10} (R = Y, La-Nd, Sm, Gd-Lu), RRu_2Al_{10} (R = Y, La-Nd, Sm, Gd, Tb, Ho, Er), ROs_2Al_{10} (R = La, Pr, Nd)	$YbFe_2Al_{10}$	$oS52$	$Cmcm$	[2]
76.1	$R_{3.64}Os_6Al_{30.69}$ (R = Nd, Sm, Gd-Yb)	$Y_{3.64}Re_6Al_{30.69}$	$hP88$-7.34	$P6_3/mcm$	[3]
75.6	$Y_{3.93}Os_6Al_{30.75}$	$Y_{3.93}Os_6Al_{30.75}$	$hP90$-8.63	$P6_3/mcm$	[4]
75.5	$NdRh_4Al_{15.37}$	$NdRh_4Al_{15.37}$	$tP96$-14.51	$P4_2/nmc$	[5]
75.0	$Ce_2Ru_3Al_{15}$	$Ce_2Ru_3Al_{15}$	$hP80$	$P6_3/mcm$	[6]
75.0	$Sm_2Os_3Al_{15}$	$Sm_2Os_3Al_{15}$	$hP84$-4.00	$P6_3/mcm$	[7]
75.0	$EuCo_2Al_9$	$BaFe_2Al_9$	$hP12$	$P6/mmm$	[8]
72.7	RFe_2Al_8 (R = La-Pr), RCo_2Al_8 (R = Pr, Sm, Yb)	$CeFe_2Al_8$	$oP44$	$Pbam$	[9]
72.6	$CeRu_{2.83}Al_{10.17}$	$CeRu_{2.83}Al_{10.17}$	$oI64$-8.00	$Imma$	[10]
70.4	$R_3Ni_5Al_{19}$ (R = Y, Gd-Tm, Lu)	$Gd_3Ni_5Al_{19}$	$oS108$	$Cmcm$	[11]
70.4	$Pr_2Co_6Al_{19}$	$U_2Co_6Al_{19}$	$mS108$	$C2/m$	[12]
70.0	La_2NiAl_7	La_2NiAl_7	$tI40$	$I4mm$	[13]
69.7	$R_4Ni_6Al_{23}$ (R = Y, Ce, Sm, Gd, Yb)	$Y_4Ni_6Al_{23}$	$mS66$	$C2/m$	[14]
69.5	$LaNi_{1.44}Al_{5.56}$	$SrAu_2Ga_5$	$tP8$	$P4/mmm$	[15]
69.2	RNi_3Al_9 (R = Gd, Er)	$ErNi_3Al_9$	$hR78$	$R32$	[16]
69.2	RNi_3Al_9 (R = Y, Dy, Yb)	$DyNi_3Al_9$	$hR99$-21.00	$R32$	[16]
66.7	$RNiAl_4$ (R = Y, Ce-Nd, Sm, Gd-Tm, Lu), $CePdAl_4$	$YNiAl_4$	$oS24$	$Cmcm$	[17]
66.7	$RCoAl_4$ (R = La-Pr)	$LaCoAl_4$	$oP12$	$Pmma$	[18]
65.2	$R_{0.67}Pt_2Al_5$ (R = Y, Ce, Gd-Er)	$Sc_{0.67}Fe_2Si_5$	$hP20$-4.67	$P6_3/mmc$	[19]
64.9	$R_{1.33}Pt_3Al_8$ (R = Ce, Gd)	$Gd_{1.33}Pt_3Al_8$	$hR51$-14.00	$R\bar{3}m$	[20]
64.9	$Er_{1.33}Pt_3Al_8$	$Er_{1.33}Pt_3Al_8$	$mS34$-9.33	$C2/m$	[21]
64.9	$R_4Pd_9Al_{24}$ (R = Gd-Tm), $R_4Pt_9Al_{24}$ (R = Gd-Lu)	$Er_4Pt_9Al_{24}$	$aP37$	$P\bar{1}$	[21]
64.9	$Y_4Pt_9Al_{24}$	$Y_4Pt_9Al_{24}$	$aP51$-14.00	$P\bar{1}$	[21]
64.3	$Y_2Co_3Al_9$, $R_2Rh_3Al_9$ (R = Y, La-Nd, Sm, Gd-Dy, Er, Tm, Lu), $R_2Pd_3Al_9$ (R = Y, Gd-Tm), $R_2Ir_3Al_9$ (R = Y, La-Nd, Sm, Gd-Ho, Tm-Lu)	$Y_2Co_3Ga_9$	$oS56$	$Cmcm$	[22]
64.3	$Ho_2Rh_3Al_9$, $Er_2Ir_3Al_9$	$Ho_2Rh_3Al_9$	$oS84$-28.00	$Cmcm$	[23]
63.2	$R_3Ru_4Al_{12}$ (R = Y, Ce-Nd, Sm, Gd-Tm), $R_3Os_4Al_{12}$ (R = Y, Ce-Nd, Sm, Gd-Tm)	$Gd_3Ru_4Al_{12}$	$hP38$	$P6_3/mmc$	[24]
62.5	RNi_2Al_5 (R = La-Pr)	$PrNi_2Al_5$	$oI16$	$Immm$	[25]
61.5	RFe_4Al_8 (R = Y, La-Nd, Sm-Lu)	$CeMn_4Al_8$	$tI26$	$I4/mmm$	[26]

$R\bar{3}m$) in [20] were used as starting model and the structure was confirmed by a full-matrix least-squares refinement using SHELXL-97. The atomic coordinates of both structures were standardized by the program STRUCTURE TIDY [29]. Crystal data and details of the data collections and structure refinements for $Tb_{0.67}PdAl_3$ and $Gd_{1.33}Pt_3Al_8$ are given in Table 2.

Results

Structure of $Tb_{0.67}PdAl_3$. The refined atomic coordinates, site occupancies, and displacement

parameters for the structure of $Tb_{0.67}PdAl_3$ are listed in Table 3. It represents a new structure type of ideal composition $R_{0.67}TAl_3$. The main feature of this structure is a statistical distribution of Tb atoms (position $2c$) and Al_3 triangles ($6h$) within atomic layers of composition $Tb_{0.67}Al$. The occupancy of the site in Wyckoff position $6h$ cannot exceed 1/3 because higher occupancy would lead to the appearance of impossibly short Al-Al distances (~1.8 Å) in the structure. Therefore, during the structure refinement, the occupancy of the Al site in Wyckoff position $6h$ was fixed at the value 0.33, whereas the occupancy of the Tb site in $2c$ was refined as a free parameter. The composition of the crystal refined to $Tb_{0.611(8)}PdAl_3$.

Table 2 Experimental details and crystallographic data for $Tb_{0.67}PdAl_3$ and $Gd_{1.33}Pt_3Al_8$.

Refined composition		$Tb_{0.611(8)}PdAl_3$	$Gd_{1.33}Pt_3Al_8$
Formula weight, M_r		284.45	1010.26
Structure type		$Tb_{0.67}PdAl_3$	$Gd_{1.33}Pt_3Al_8$
Pearson symbol		hP14-4.67	hR51-14.00
Space group		$P6_3/mmc$ (#194)	$R\bar{3}m$ (#166)
Unit-cell parameters:	a, Å	4.394(4)	4.3090(14)
	c, Å	9.372(6)	38.54(2)
Cell volume V, Å^3		156.7(2)	619.7(5)
Formula units per cell Z		2	3
Density D_X, g cm^{-3}		6.029	8.121
Absorption coefficient μ, mm^{-1}		20.013	61.951
Crystal shape		prism	plate
Crystal size, mm		0.035×0.035×0.100	0.055×0.055×0.035
Color		metallic grey	metallic grey
# of reflections:	measured	1041	710
	independent	119	345
	with $I > 2\sigma(I)$	87	227
Reliability factor R_{int}		0.0813	0.0445
Range of h, k, l		$-6 \le h \le 5$, $-3 \le k \le 6$, $-13 \le l \le 13$	$-5 \le h \le 1$, $-5 \le k \le 2$, $-54 \le l \le 54$
Range θ, º		4.35-30.47	4.76-30.47
Reliability factors:	R	0.0316	0.0641
	wR	0.0650	0.1398
	S	1.353	1.355
# of reflections used in refinement		87	227
# of refined parameters		13	24
Weighting scheme		$w = 1/[(\sigma F_o)^2 +$	$w = 1/[(\sigma F_o)^2 +$
$(P = (F_o^2 + 2F_c^2)/3)$		$(0.0186P)^2 + 1.77P]$	$(0.0610P)^2 + 97.70P]$
Residual electron density:	$\Delta\rho_{max}$, e Å^{-3}	1.513	6.357
	$\Delta\rho_{min}$, e Å^{-3}	-2.029	-6.079

Table 3 Atomic coordinates, site occupancies, and displacement parameters (Å^2) for $Tb_{0.67}PdAl_3$ (hP14-4.67, $P6_3/mmc$, a = 4.394(4), c = 9.372(6) Å).

Site	Wyckoff position	x	y	z	U_{eq}	Occupancy
Tb	2c	⅓	⅔	¼	0.0074(7)	0.611(8)
Pd	2a	0	0	0	0.0097(6)	1
Al1	6h	0.134(2)	0.268(4)	¼	0.014(3)	0.33
Al2	4f	⅓	⅔	0.5727(6)	0.0144(11)	1

Site	U_{11}	U_{22}	U_{33}	U_{12}	U_{13}	U_{23}
Tb	0.0079(8)	0.0079(8)	0.0065(8)	0.0039(4)	0	0
Pd	0.0103(8)	0.0103(8)	0.0087(9)	0.0051(4)	0	0
Al1	0.015(5)	0.032(9)	0.000(4)	0.016(5)	0	0
Al2	0.0066(15)	0.0066(15)	0.030(3)	0.0033(8)	0	0

The content of the unit cell and the coordination polyhedra in the structure of $Tb_{0.67}PdAl_3$ are shown in Fig. 1, and the interatomic distances within the coordination polyhedra are listed in Table 4. The Tb atoms center 20-vertex polyhedra [TbAl$_{11}$Pd$_6$Tb$_3$], which can be described as hexagonal prisms of composition Al$_6$Pd$_6$ with three Tb and five additional Al atoms capping the eight faces. The smaller atoms are characterized by icosahedral coordination: [PdAl$_8$Tb$_4$] (can also be described as a deformed cuboctahedron), [Al1Al$_8$Pd$_2$Tb$_2$] and strongly

deformed [Al2Al$_6$Pd$_3$Tb$_3$]. These polyhedra are very similar to those observed in the structure type $Y_2Co_3Ga_9$ [22], which is an ordered variant of the $Tb_{0.67}PdAl_3$ structure with fully ordered distribution of rare-earth-metal atoms and p-element-atom triangles.

Structure of $Gd_{1.33}Pt_3Al_8$. $Gd_{1.33}Pt_3Al_8$ crystallizes with its own structure type; our refinements confirm the structural model proposed in [20]. The refined atomic coordinates, site occupancies, and displacement parameters are listed in Table 5. As for the structure of the $Tb_{0.67}PdAl_3$ compound, the main feature of the

Table 4 Interatomic distances for $Tb_{0.67}PdAl_3$ (hP14-4.67, $P6_3/mmc$, $a = 4.394(4)$, $c = 9.372(6)$ Å).

Atoms		δ, Å
Tb[a]	– 2 Al2	3.025(6)
	– 6 Al2	3.032(4)
	– 3 Al1[b]	3.171(12)
	– 6 Pd	3.4532(19)
	– 3 Tb[a]	4.394(4)
Pd	– 2 Al1[b]	2.555(7)
	– 6 Al2	2.627(3)
	– 4 Tb[a]	3.4532(19)
Al1[b]	– 2 Pd	2.555(7)
	– 2 Al1[b]	2.63(3)
	– 4 Al2	2.765(4)
	– 2 Tb[f]	3.171(12)
	– 2 Al2	3.384(9)
Al2	– 3 Pd	2.627(3)
	– 2 Al1[b]	2.765(4)
	– 3 Al2	2.880(6)
	– 1 Tb[a]	3.025(6)
	– 2 Tb[a]	3.032(4)
	– 1 Al2	3.322(11)
	[– 3 Al1[b]	3.384(9)]

[a] occ. (Tb) = 0.611(8); [b] occ. (Al1) = 0.33

Table 5 Atomic coordinates, site occupancies, and displacement parameters (Å²) for $Gd_{1.33}Pt_3Al_8$ (hR51-14.00, $R\bar{3}m$, $a = 4.3090(14)$, $c = 38.54(2)$ Å).

Site	Wyckoff position	x	y	z	U_{eq}	Occupancy
Gd	$6c$	0	0	0.26941(10)	0.0034(8)	0.67
Pt1	$6c$	0	0	0.12093(5)	0.0037(6)	1
Pt2	$3a$	0	0	0	0.0106(8)	1
Al1	$18h$	0.539(4)	0.461(4)	0.3947(7)	0.011(5)	0.33
Al2	$6c$	0	0	0.1872(4)	0.006(3)	1
Al3	$6c$	0	0	0.3514(5)	0.010(3)	1
Al4	$6c$	0	0	0.4437(4)	0.006(3)	1

| Site	U_{11}	U_{22}	U_{33}	U_{12}	U_{13}	U_{23}
Gd	0.0025(11)	0.0025(11)	0.0052(18)	0.0012(6)	0	0
Pt1	0.0039(7)	0.0039(7)	0.0033(9)	0.0020(3)	0	0
Pt2	0.0100(10)	0.0100(10)	0.0117(15)	0.0050(5)	0	0
Al1	0.007(7)	0.007(7)	0.007(11)	-0.005(9)	-0.006(5)	0.006(5)
Al2	0.006(5)	0.006(5)	0.005(6)	0.003(2)	0	0
Al3	0.006(5)	0.006(5)	0.017(10)	0.003(2)	0	0
Al4	0.007(4)	0.007(4)	0.003(7)	0.004(2)	0	0

structure of $Gd_{1.33}Pt_3Al_8$ is a statistical distribution of R atoms and Al_3 triangles within atomic layers of composition $R_{0.67}Al$. During the final cycles of the refinement, the occupancies of the corresponding sites were fixed at occ. = 0.67 for Gd in $6c$ and occ. = 0.33 for Al in $18h$.

The content of the unit cell and the coordination polyhedra in the structure of $Gd_{1.33}Pt_3Al_8$ are shown in Fig. 2, and the interatomic distances within the coordination polyhedra are listed in Table 6. As in the

structure of $Tb_{0.67}PdAl_3$, the large atoms (Gd) center the 20-vertex polyhedra [$\underline{Gd}Al_{11}Pt_6Gd_3$] (hexagonal prisms of composition Al_6Pt_6 with three Gd and five additional Al atoms capping the eight faces). The coordination polyhedra around the Pt and Al atoms are icosahedra, or derivatives of these with one or two missing vertices: [$\underline{Pt1}Al_8Gd_2$] (defect icosahedron or cuboctahedron), [$\underline{Pt2}Al_8Gd_4$] (or cuboctahedron), [$\underline{Al1}Al_8Pt_2Gd_2$], [$\underline{Al2}Al_6Pt_4Gd$] (defect), [$\underline{Al3}Al_6Pt_3Gd_3$], [$\underline{Al4}Al_6Pt_3Gd_2$] (defect).

Table 6 Interatomic distances for $Gd_{1.33}Pt_3Al_8$ ($hR51$-14.00, $R\bar{3}m$, $a = 4.3090(14)$, $c = 38.54(2)$ Å).

Atoms		δ, Å	Atoms		δ, Å
Gd[a]	– 3 Al3	3.051(11)	Al2	– 1 Pt1	2.553(16)
	– 3 Al4	3.064(10)		– 3 Pt1	2.671(6)
	– 3 Al1[b]	3.08(2)		– 3 Al4	2.845(11)
	– 1 Al3	3.160(19)		– 3 Al2	2.948(17)
	– 1 Al2	3.169(16)		– 1 Gd[a]	3.169(16)
	– 3 Pt1	3.319(3)		[– 3 Al1[b]	3.61(3)]
	– 3 Pt2	3.501(3)	Al3	– 3 Pt2	2.583(5)
	– 3 Gd[a]	4.3090(14)		– 2 Al1[b]	2.742(19)
Pt1	– 1 Al1[b]	2.48(3)		– 3 Al3	2.851(18)
	– 3 Al4	2.521(3)		– 2 Gd[a]	3.051(11)
	– 1 Al2	2.553(16)		– 1 Gd[a]	3.160(19)
	– 3 Al2	2.671(6)		[– 3 Al1[b]	3.43(3)]
	– 2 Gd[a]	3.319(3)		– 1 Al4	3.56(3)
Pt2	– 2 Al1[b]	2.55(3)	Al4	– 3 Pt1	2.521(3)
	– 6 Al3	2.583(5)		– 3 Al2	2.845(11)
	– 4 Gd[a]	3.501(3)		– 2 Al1[b]	2.88(2)
Al1[b]	– 1 Pt1	2.48(3)		– 2 Gd[a]	3.064(10)
	– 1 Pt2	2.55(3)		– 1 Al3	3.56(3)
	– 2 Al1[b]	2.66(6)			
	– 2 Al3	2.742(19)			
	– 2 Al4	2.88(2)			
	– 2 Gd[a]	3.08(2)			
	– 1 Al3	3.43(3)			
	– 1 Al2	3.61(3)			

[a] occ. (Gd) = 0.67; [b] occ. (Al1) = 0.33
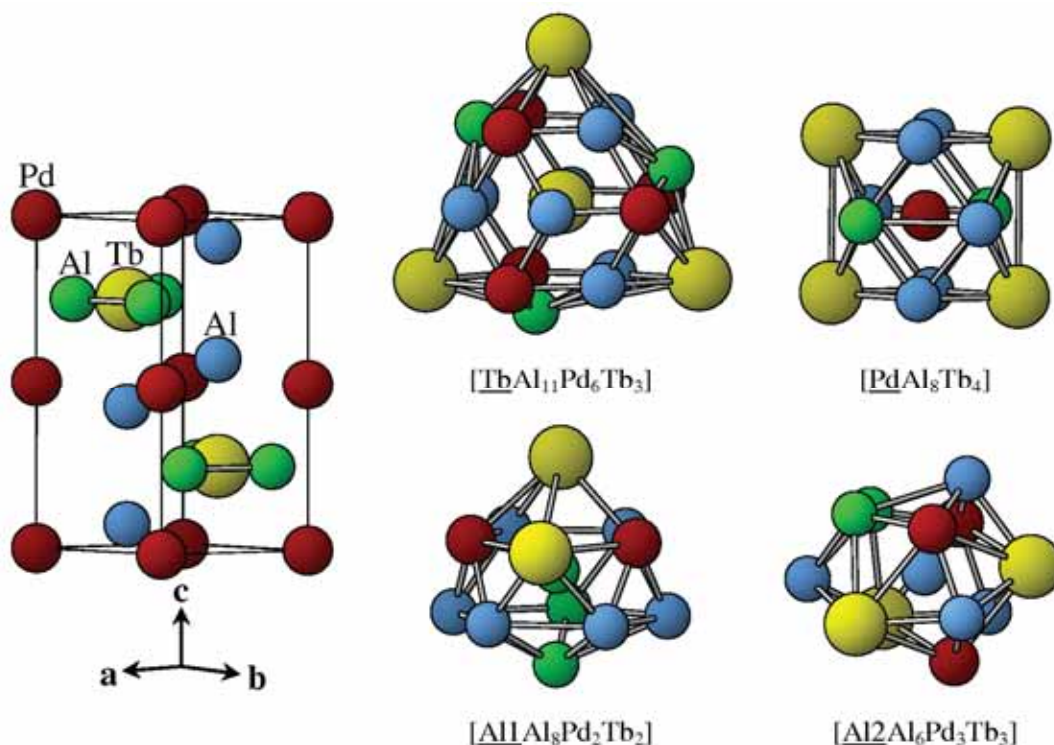
Fig. 1 The unit cell and coordination polyhedra for atoms in the $Tb_{0.67}PdAl_3$ structure.
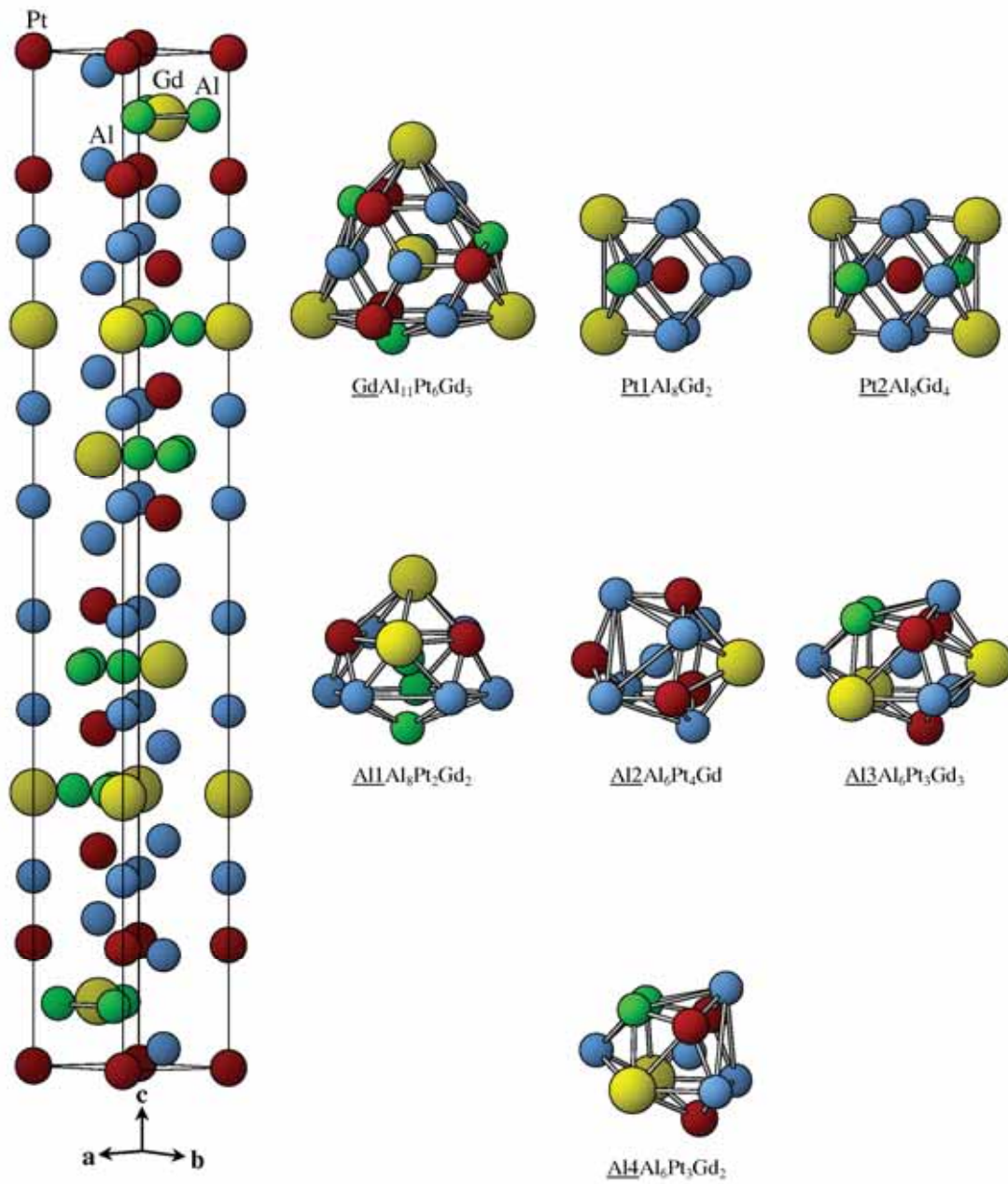
Fig. 2 The unit cell and coordination polyhedra for atoms in the $Gd_{1.33}Pt_3Al_8$ structure.
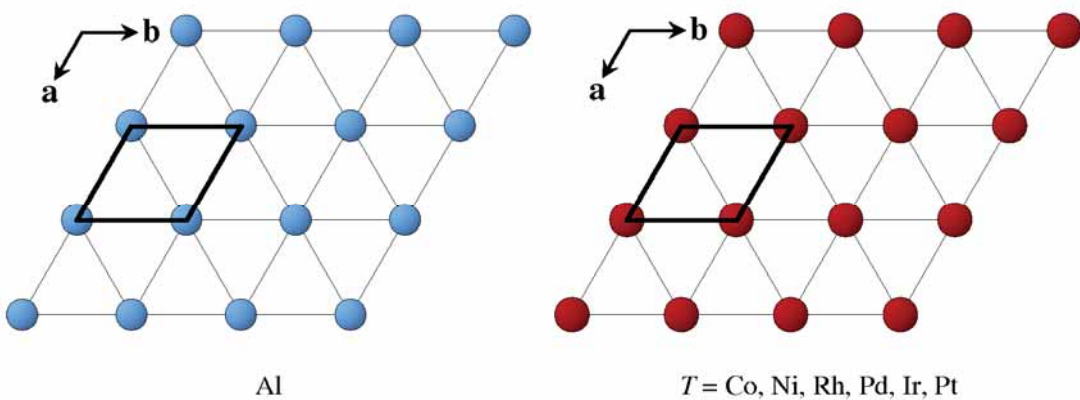

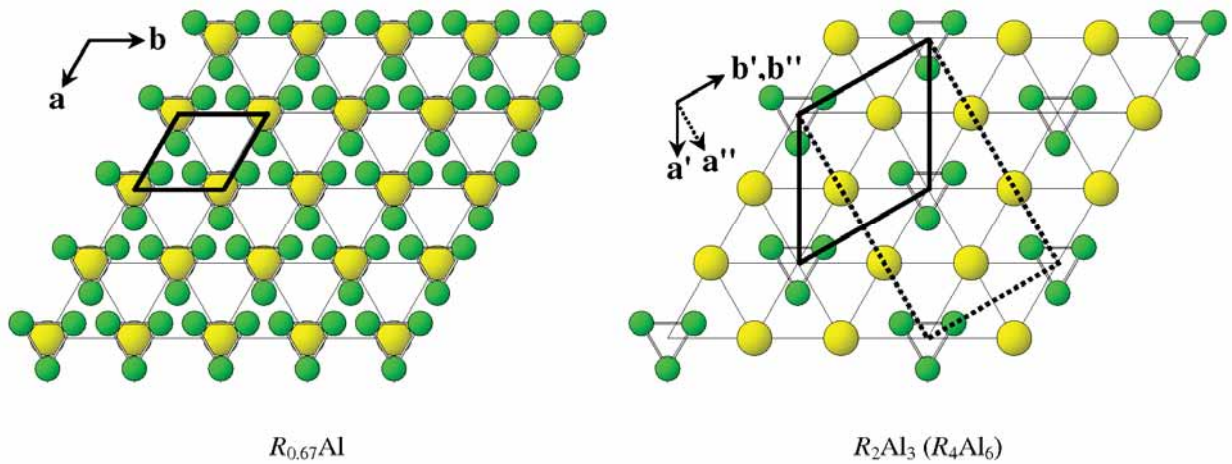**Fig. 3** Monoatomic Al- and *T*-atom layers with triangular meshes.

Fig. 4 Monoatomic $R_{0.67}Al \equiv R_2Al_3 \equiv R_4Al_6$ layers: disordered and ordered distribution of R atoms and Al_3 triangles.
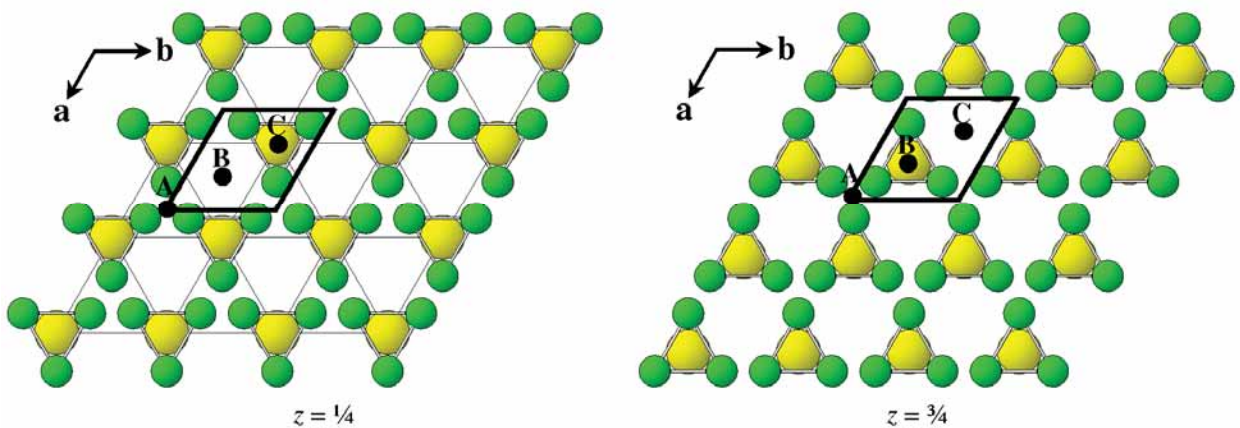

Fig. 5 Monoatomic $Tb_{0.67}Al$ layers in the $Tb_{0.67}PdAl_3$ structure.

Discussion

Three kinds of monoatomic (one-atom thick) layer can be considered in the structure types $Tb_{0.67}PdAl_3$, $Y_2Co_3Ga_9$ [22], $Sc_{0.67}Fe_2Si_5$ [19], $Gd_{1.33}Pt_3Al_8$ [20], $Er_4Pt_9Al_{24}$ [21], $R_{0.67}Ni_2Al_6$ (hypothetic) [16], and $ErNi_3Al_9$ [16]. Two of them have triangular mesh, *i.e.* they possess the motif of close-packed layers, but the interatomic distances within the layers for aluminides (see Table 1) are ~4.3 Å. Such layers formed by *p*- (Al) or *d*-element atoms (T = Co, Ni, Rh, Pd, Ir, Pt) are shown in Fig. 3. The third kind of layer has the composition $R_{0.67}Al \equiv R_2Al_3 \equiv R_4Al_6$ (R = rare-earth metal). The R atoms and the centers of Al_3 triangles also form a triangular mesh (Fig. 4). These layers derive from close-packed R-atom layers by a statistical (disordered) or ordered replacement of one-third of the R atoms by Al_3 triangles. In case of ordered substitution, the translation unit for such layers will be three times larger (new parameters: $\mathbf{a'} = 2\mathbf{a} + \mathbf{b}$, $\mathbf{b'} = -\mathbf{a} + \mathbf{b}$, see Fig. 4). The monoatomic layers are stacked along the crystallographic direction [001] in all the above mentioned structure types, *i.e.* they are perpendicular to the 6-fold axes in the hexagonal structures and 3-fold axes in the trigonal (rhombohedral) structures. The ratio of different layers, the stacking sequence and the degree of ordering in the R_2Al_3 layers distinguish the different structure types. The interatomic distances within triangles (~2.65 Å) are the shortest Al-Al contacts in the structures indicating strong interaction.

For the comparison and discussion of the above mentioned structures we use the conventional symbols introduced to define the stacking sequence of monoatomic layers in close-packed structures: position **A** with coordinates $x = 0$, $y = 0$, **B** with $x = \frac{2}{3}$, $y = \frac{1}{3}$ and **C** with $x = \frac{1}{3}$, $y = \frac{2}{3}$ (referring to the small hexagonal translation unit).

$z = -0.0726$
$z = 0.0726$
$z = 0$

$z = -0.0726\text{-}0.0726$
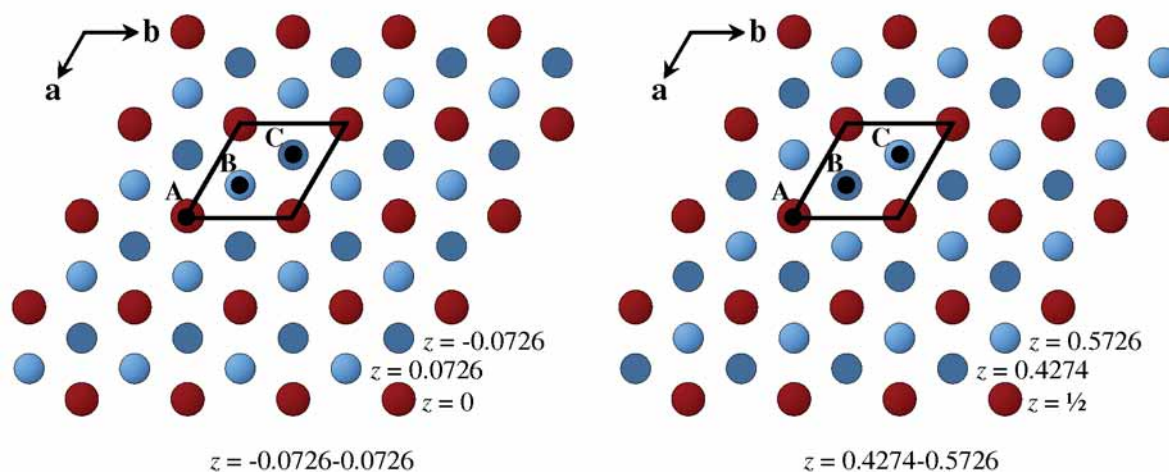
$z = 0.5726$
$z = 0.4274$
$z = \frac{1}{2}$

$z = 0.4274\text{-}0.5726$

Fig. 6 Monoatomic Pd- and Al-atom layers in the $Tb_{0.67}PdAl_3$ structure.

The hexagonal unit cell of $Tb_{0.67}PdAl_3$ contains eight monoatomic layers along the crystallographic direction [001]: two layers of composition $Tb_{0.67}Al$ (at $z = \frac{1}{4}$ and $\frac{3}{4}$), two Pd layers ($z = 0$ and $\frac{1}{2}$) and four Al layers ($z = 0.0726$, 0.4274, 0.5726, and 0.9274). The composition of the compound can be written as $2Tb_{0.67}Al + 2Pd + 4Al = 2Tb_{0.67}PdAl_3$. In Figs. 5 and 6, the $Tb_{0.67}Al$ layer at $z = \frac{1}{4}$ has been assigned the relative stacking position **C**, whereas the $Tb_{0.67}Al$ layer at $z = \frac{3}{4}$ is shifted to position **B**; both Pd layers ($z = 0$ and $\frac{1}{2}$) are located in the relative position **A**, two of the Al layers ($z = 0.0726$ and 0.4274) in **B**, and the remaining Al layers ($z = 0.5726$ and 0.9274) in position **C**. Hence, the structure of the $Tb_{0.67}PdAl_3$ compound is characterized by the following stacking sequence of monoatomic layers: **A**(Pd)-**B**(Al)-**C**($Tb_{0.67}Al$)-**B**(Al)-**A**(Pd)-**C**(Al)-**B**($Tb_{0.67}Al$)-**C**(Al). Standardization of the symbols assigned to the relative positions of the monoatomic layers so that the $Tb_{0.67}Al$ layer at $z = \frac{1}{4}$ is located in position **A**, leads to the following stacking sequence: **B**(T)-**C**(Al)-**A**($R_{0.67}Al$)-**C**(Al)-**B**(T)-**A**(Al)-**C**($R_{0.67}Al$)-**A**(Al) (Fig. 7).

The structures of the $R_2T_3Al_9$ compounds (T = Co, Rh, Pd, Ir) adopting the $Y_2Co_3Ga_9$ type have cell parameters c similar to that of $Tb_{0.67}PdAl_3$ and contain eight monoatomic layers stacked in the same way along [001]: **B**(T_6)-**C**(Al_6)-**A**(R_4Al_6)-**C**(Al_6)-**B**(T_6)-**A**(Al_6)-**C**(R_4Al_6)-**A**(Al_6) (Fig. 8). However, contrary to $Tb_{0.67}PdAl_3$, in the structure of $R_2T_3Al_9$ the R atoms and Al_3 triangles are distributed in an ordered way, leading to orthorhombic symmetry with a six times larger cell volume. Thus, the $Y_2Co_3Ga_9$ type is an ordered derivative of $Tb_{0.67}PdAl_3$. The group-subgroup relation for the corresponding space groups is the following: $P6_3/mmc$ (**a**, **b**, **c**) $\xrightarrow{IIb}$ $P6_3/mcm$ (**a'** $= 2$**a** $+$ **b**, **b'** $= -$**a** $+$ **b**, **c'** $=$ **c**) $\xrightarrow{I}$ $Cmcm$ (**a''** $= 2$**a'** $+$ **b'**, **b''** $= 2$**b'**, **c''** $=$ **c'**) [27]. Complete ordering of R atoms and Al_3 triangles is not possible in the intermediate superstructure with three-fold cell volume and space group $P6_3/mcm$, since only one Wyckoff position is available for the rare-earth-metal

atoms. Orthorhombic $Ho_2Rh_3Al_9$ is a partly disordered variant of $Y_2Co_3Ga_9$.

The $R_{0.67}Pt_2Al_5$ compounds belonging to the hexagonal $Sc_{0.67}Fe_2Si_5$ type and the trigonal (rhombohedral) $Gd_{1.33}Pt_3Al_8$-type compounds also contain disordered $R_{0.67}Al$ layers. The unit cell of the $Sc_{0.67}Fe_2Si_5$ type contains 14 monoatomic layers along the crystallographic direction [001] (Fig. 9): two $R_{0.67}Al$ layers, four T layers and eight Al layers. The composition of the corresponding compounds may be written in the following way: $2R_{0.67}Al + 4T + 8Al = 2R_{0.67}T_2Al_5$. The $Sc_{0.67}Fe_2Si_5$ type is described by the stacking sequence **A**(Al)-**B**(T)-**C**(Al)-**A**($R_{0.67}Al$)-**C**(Al)-**B**(T)-**A**(Al)-**B**(Al)-**A**(T)-**C**(Al)-**B**($R_{0.67}Al$)-**C**(Al)-**A**(T)-**B**(Al). Ordered derivatives of the $Sc_{0.67}Fe_2Si_5$ type are not yet known.

The unit cell of the structure of $Gd_{1.33}Pt_3Al_8$ contains six $R_{0.67}Al$ layers, nine T and eighteen Al layers along the crystallographic direction [001] (Fig. 10). The composition is $6R_{0.67}Al + 9T + 18Al = 3R_{1.33}T_3Al_8$, and the 33 monoatomic layers are stacked in the following way in the triple hexagonal cell: **A**(T)-**C**(Al)-**B**($R_{0.67}Al$)-**C**(Al)-**A**(T)-**B**(Al)-**A**(Al)-**B**(T)-**C**(Al)-**A**($R_{0.67}Al$)-**C**(Al)-**B**(T)-**A**(Al)-**C**($R_{0.67}Al$)-**A**(Al)-**B**(T)-**C**(Al)-**B**(Al)-**C**(T)-**A**(Al)-**B**($R_{0.67}Al$)-**A**(Al)-**C**(T)-**B**(Al)-**A**($R_{0.67}Al$)-**B**(Al)-**C**(T)-**A**(Al)-**C**(Al)-**A**(T)-**B**(Al)-**C**($R_{0.67}Al$)-**B**(Al). In fact, the structure of $Gd_{1.33}Pt_3Al_8$ is an intergrowth of $Tb_{0.67}PdAl_3$- and $Sc_{0.67}Fe_2Si_5$-type slabs (in the ratio 1:1) delimited by the $R_{0.67}Al$ layers. Such an intergrowth leads to rhombohedral symmetry. Triclinic $Er_4Pt_9Al_{24}$ is an ordering variant of $Gd_{1.33}Pt_3Al_8$ (R atoms and Al_3 triangles are distributed orderly) and its cell contains along the stacking direction [$\bar{1}$01] 11 monoatomic layers in the sequence: **C**(T_3)-**B**(Al_3)-**A**(R_2Al_3)-**B**(Al_3)-**C**(T_3)-**A**(Al_3)-**C**(Al_3)-**A**(T_3)-**B**(Al_3)-**C**(R_2Al_3)-**B**(Al_3) (Fig. 11). The transformation from the triple hexagonal cell of $Gd_{1.33}Pt_3Al_8$ to the triclinic cell of $Er_4Pt_9Al_{24}$ is following: **a'** $= 2$**a** $+$ **b**, **b'** $=$ **a** $+ 2$**b**, **c'** $= 2$**a**/3 $+$ **b**/3 $+$ **c**/3.
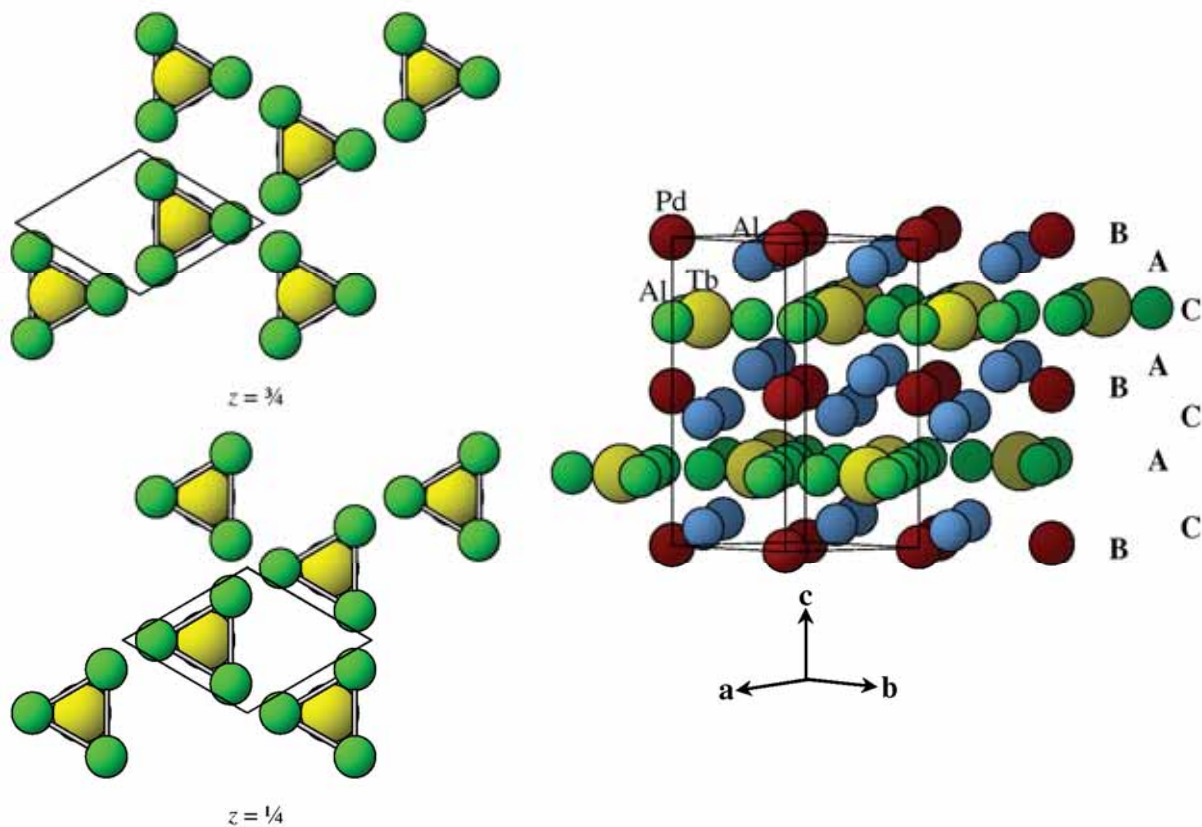
Fig. 7 Stacking of monoatomic layers along [001] and $R_{0.67}M$ layers in the $Tb_{0.67}PdAl_3$ structure.
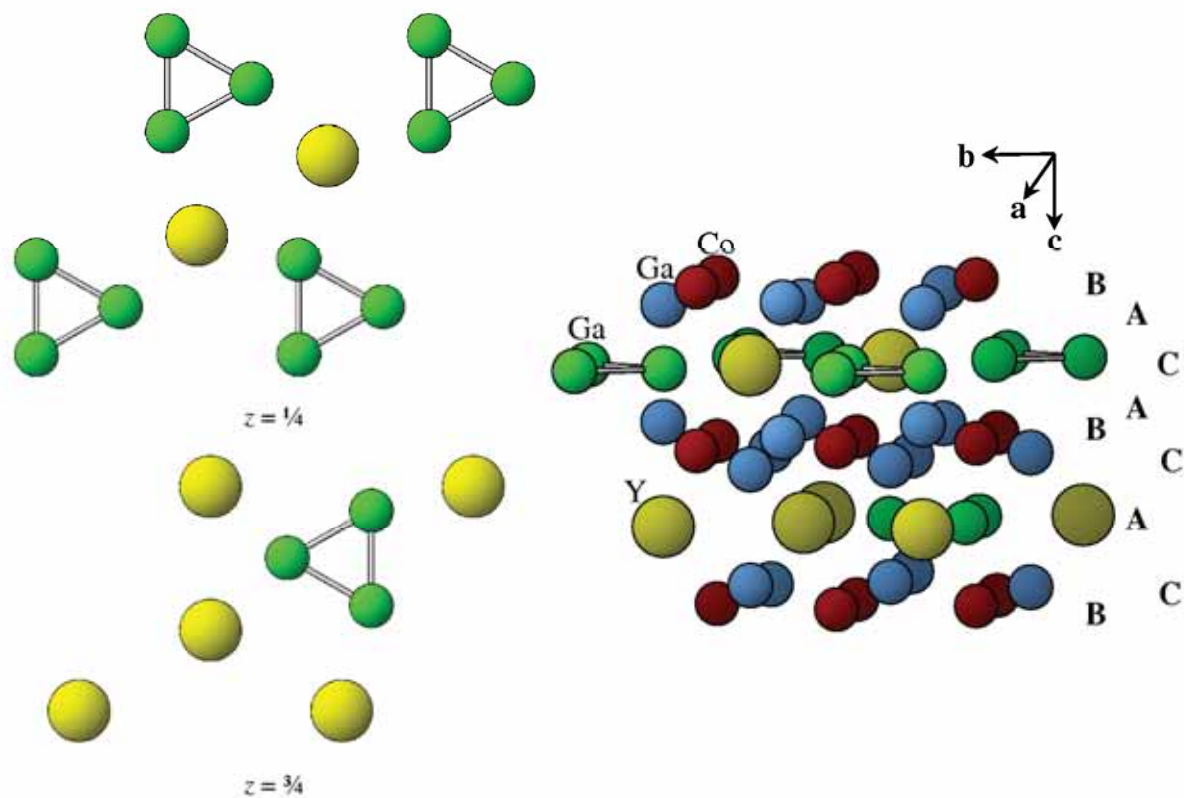

Fig. 8 Stacking of monoatomic layers along [001] and R_4M_6 layers in an $Y_2Co_3Ga_9$-type structure.
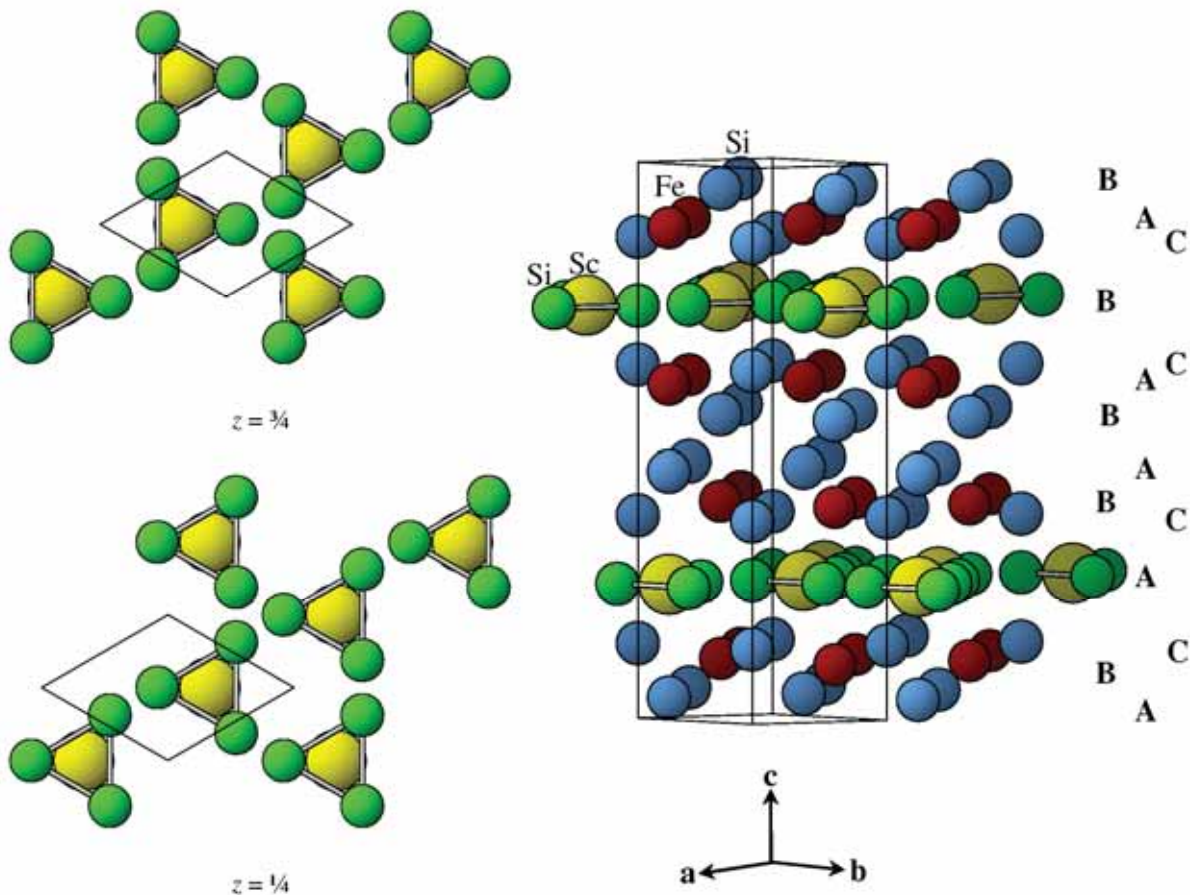
Fig. 9 Stacking of monoatomic layers along [001] and $R_{0.67}M$ layers in an $Sc_{0.67}Fe_2Si_5$-type structure.

Monoclinic $Er_{1.33}Pt_3Al_8$ (transformation from $Gd_{1.33}Pt_3Al_8$: $\mathbf{a'} = 2\mathbf{a} + \mathbf{b}$, $\mathbf{b'} = \mathbf{b}$, $\mathbf{c'} = -2\mathbf{a}/3 - \mathbf{b}/3 + \mathbf{c}/3$) and triclinic $Y_4Pt_9Al_{24}$ (transformation from $Gd_{1.33}Pt_3Al_8$ as for $Er_4Pt_9Al_{24}$) differ from $Er_4Pt_9Al_{24}$ by a partly disordered distribution of R atoms and Al_3 triangles.

Along the translation period c of the triple hexagonal cell of the trigonal (rhombohedral) structure type $ErNi_3Al_9$ there are 24 monoatomic layers: three R_2Al_3, six T_3 and fifteen Al_3; consequently, the composition of the compound is $3R_2Al_3 + 6T_3 + 15Al_3 = 6RT_3Al_9$. The stacking sequence of the monoatomic layers repeats three times in the unit cell (Fig. 12): $\mathbf{B}(Al_3)$-$\mathbf{A}(Al_3)$-$\mathbf{B}(T_3)$-$\mathbf{C}(Al_3)$-$\mathbf{A}(R_2Al_3)$-$\mathbf{C}(Al_3)$-$\mathbf{B}(T_3)$-$\mathbf{A}(Al_3)$, and the rhombohedral Bravais lattice is the result of a relative shift of the Al_3 triangles in consecutive R_2Al_3 layers. Trigonal (rhombohedral) $DyNi_3Al_9$ differs from $ErNi_3Al_9$ by the distribution of R atoms and Al_3 triangles: in the $ErNi_3Al_9$ structure it is fully ordered, whereas in the structure of $DyNi_3Al_9$ it is partially disordered. The structure types $ErNi_3Al_9$ and $DyNi_3Al_9$ derive from a hypothetical hexagonal structure of composition $R_{0.67}Ni_2Al_6$ ($hP11$-2.33, $P\bar{6}m2$, $a \approx 4.20$, $c \approx 9.12$ Å [16]) with maximal disorder of R atoms and Al_3 triangles. The unit cell volume of the $R_{0.67}Ni_2Al_6$

structure is nine times smaller than the volume of the triple hexagonal cells of the $ErNi_3Al_9$ and $DyNi_3Al_9$ types ($\mathbf{a'} = 2\mathbf{a}/3 + \mathbf{b}/3$, $\mathbf{b'} = -\mathbf{a}/3 + \mathbf{b}/3$, $\mathbf{c'} = \mathbf{c}/3$).

The stacking sequences of the monoatomic layers in the structure types discussed above are summarized in Table 7. For each type of layer, $R_{0.67}Al \equiv R_2Al_3 \equiv R_4Al_6$, $T \equiv T_3 \equiv T_6$, $Al \equiv Al_3 \equiv Al_6$, the symbols of their relative positions (**A**, **B**, **C**) and the Jagodzinski-Wyckoff symbols (***h***, ***c***) [29] are listed. Based on the analysis of the known structures, some general rules for the stacking of the monoatomic layers in structures containing layers with ordered or disordered distribution of R atoms and Al_3 triangles can be deduced:

- an $R_{0.67}Al$ layer is always located in hexagonal stacking (***h***) between two Al layers;
- a T layer is always located in cubic stacking (***c***) between two Al layers;
- $R_{0.67}Al$ and T layers are bridged by a single Al layer in cubic (***c***) stacking;
- T layers are separated by one or several Al layers in hexagonal (***h***) stacking.

The degree of hexagonal stacking (hexagonality) increases with increasing Al content: 25% of hexagonal stacking for $Tb_{0.67}PdAl_3$ and $Y_2Co_3Ga_9$-type aluminides (64.3 at.% Al), 36.4% for $Gd_{1.33}Pt_3Al_8$

Table 7 Stacking sequences of monoatomic layers in structures containing $R_{0.67}Al$ layers.

Structure type	Stacking sequence[a]																								
$Tb_{0.67}PdAl_3$, $Y_2Co_3Ga_9$	*R*	*M*	*T*	*M*	*R*	*M*	*T*	*M*	*R*	*M*	*T*	*M*	*R*	*M*	*T*	*M*	*R*	*M*	*T*	*M*	*R*	*M*	*T*	*M*	*R*
	C	**A**	**B**	**C**	**A**	**C**	**B**	**A**	**C**	**A**	**B**	**C**	**A**	**C**	**B**	**A**	**C**	**A**	**B**	**C**	**A**	**C**	**B**	**A**	**C**
	h	*c*	*c*	*c*	*h*	*c*	*c*	*c*	*h*	*c*	*c*	*c*	*h*	*c*	*c*	*c*	*h*	*c*	*c*	*c*	*h*	*c*	*c*	*c*	*h*
$Sc_{0.67}Fe_2Si_5$	*T*	*M*	*M*	*T*	*M*	*R*	*M*	*T*	*M*	*M*	*T*	*M*	*R*	*M*	*T*	*M*	*M*	*T*	*M*	*R*	*M*	*T*	*M*	*M*	*T*
	B	**A**	**B**	**A**	**C**	**B**	**C**	**A**	**B**	**A**	**B**	**C**	**A**	**C**	**B**	**A**	**B**	**A**	**C**	**B**	**C**	**A**	**B**	**A**	**B**
	c	*h*	*h*	*c*	*c*	*h*	*c*	*c*	*h*	*h*	*c*	*c*	*h*	*c*	*c*	*h*	*h*	*c*	*c*	*h*	*c*	*c*	*h*	*h*	*c*
$Gd_{1.33}Pt_3Al_8$, $Er_4Pt_9Al_{24}$	*M*	*R*	*M*	*T*	*M*	*R*	*M*	*T*	*M*	*M*	*T*	*M*	*R*	*M*	*T*	*M*	*R*	*M*	*T*	*M*	*M*	*T*	*M*	*R*	*M*
	B	**C**	**B**	**A**	**C**	**B**	**C**	**A**	**B**	**A**	**B**	**C**	**A**	**C**	**B**	**A**	**C**	**A**	**B**	**C**	**B**	**C**	**A**	**B**	**A**
	c	*h*	*c*	*c*	*c*	*h*	*c*	*c*	*h*	*h*	*c*	*c*	*h*	*c*	*c*	*c*	*h*	*c*	*c*	*h*	*h*	*c*	*c*	*h*	*c*
$R_{0.67}Ni_2Al_6$, $ErNi_3Al_9$	*M*	*M*	*T*	*M*	*R*	*M*	*T*	*M*	*M*	*M*	*T*	*M*	*R*	*M*	*T*	*M*	*M*	*M*	*T*	*M*	*R*	*M*	*T*	*M*	*M*
	B	**A**	**B**	**C**	**A**	**C**	**B**	**A**	**B**	**A**	**B**	**C**	**A**	**C**	**B**	**A**	**B**	**A**	**B**	**C**	**A**	**C**	**B**	**A**	**B**
	h	*h*	*c*	*c*	*h*	*c*	*c*	*h*	*h*	*h*	*c*	*c*	*h*	*c*	*c*	*h*	*h*	*h*	*c*	*c*	*h*	*c*	*c*	*h*	*h*

[a] R – layer of composition $R_{0.67}Al \equiv R_2Al_3 \equiv R_4Al_6$ (R = rare-earth metal), $T – T \equiv T_3 \equiv T_6$ (T = Co, Ni, Rh, Pd, Ir, Pt), $M – M \equiv M_3 \equiv M_6$ (M = Al); **A**, **B**, **C** – relative shift of the layer perpendicular to the stacking direction; *h*, *c* – Jagodzinski-Wyckoff symbol
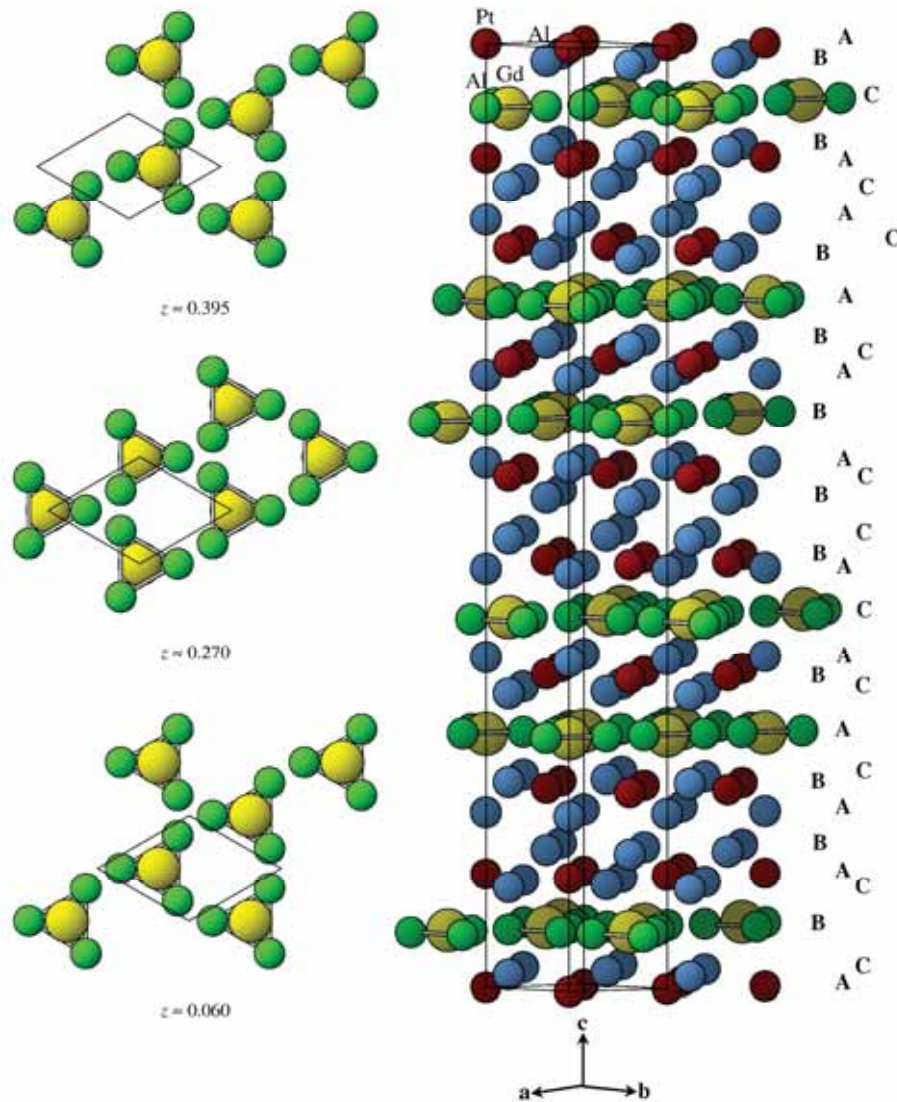

Fig. 10 Stacking of monoatomic layers along [001] and $R_{0.67}M$ layers in the $Gd_{1.33}Pt_3Al_8$ structure.
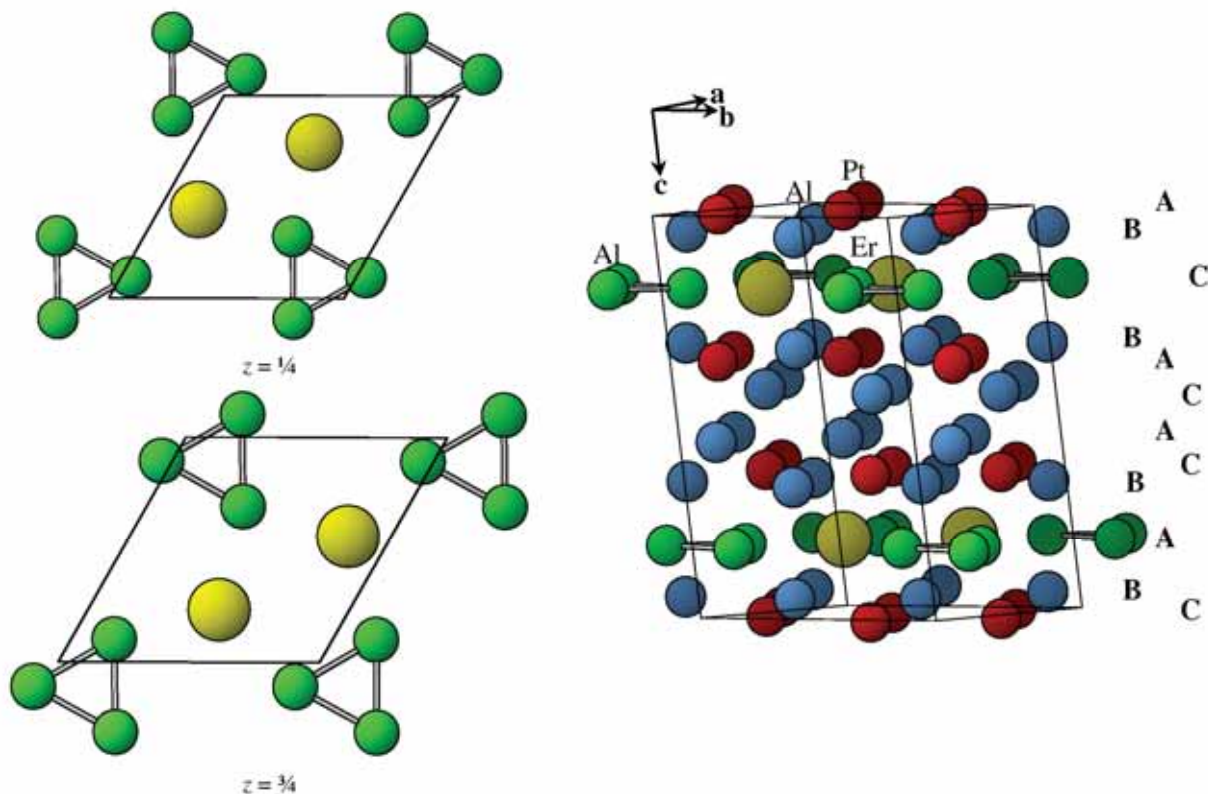
Fig. 11 Stacking of monoatomic layers along [001] and R_2M_3 layers in the $Er_4Pt_9Al_{24}$ structure.

Table 8 Members of the homologous series $R_{0.67}T_nM_{2n+m}$.

Structure type	Space group	Slabs			Ideal composition
		$R_{0.67}M$	MTM	M	
$Tb_{0.67}PdAl_3$	$P6_3/mmc$	2	2	–	$2R_{0.67}TM_3$
$Y_2Co_3Ga_9$	$Cmcm$	$2(R_4M_6)$	$2(M_6T_6M_6)$	–	$12R_{0.67}TM_3 \equiv 4R_2T_3M_9$
$Sc_{0.67}Fe_2Si_5$	$P6_3/mmc$	2	4	–	$2R_{0.67}T_2M_5$
$Gd_{1.33}Pt_3Al_8$	$R\bar{3}m$	6	9	–	$6R_{0.67}T_{1.5}M_4 \equiv 3R_{1.33}T_3M_8$
$Er_4Pt_9Al_{24}$	$P\bar{1}$	$2(R_2M_3)$	$3(M_3T_3M_3)$	–	$6R_{0.67}T_{1.5}M_4 \equiv R_4T_9M_{24}$
$R_{0.67}Ni_2Al_6$	$P\bar{6}m2$	1	2	1	$R_{0.67}T_2M_6$
$ErNi_3Al_9$	$R32$	$3(R_2M_3)$	$6(M_3T_3M_3)$	$3(M_3)$	$9R_{0.67}T_2M_6 \equiv 6RT_3M_9$

(64.9 at.% Al), 42.9% for $Sc_{0.67}Fe_2Si_5$-type aluminides (65.2 at.% Si), and 50% for $R_{0.67}Ni_2Al_6$ and $ErNi_3Al_9$ (69.2 at.% Al).

Since a *T* layer is always surrounded by two Al (*M*) layers, it is possible to consider slabs formed by three consecutive layers Al-*T*-Al (*MTM* slabs). The structure types $Tb_{0.67}PdAl_3$, $Y_2Co_3Ga_9$, $Sc_{0.67}Fe_2Si_5$, $Gd_{1.33}Pt_3Al_8$, $Er_4Pt_9Al_{24}$, $R_{0.67}Ni_2Al_6$, and $ErNi_3Al_9$ form a homologous series with the general formula $R_{0.67}T_nM_{2n+m}$, based on the stacking of three different structural slabs. Two of them are identical to the monoatomic $R_{0.67}M$ and M layers discussed above, whereas the third one is the *MTM* slab. In the structure of $Tb_{0.67}PdAl_3$ (as well as in $Y_2Co_3Ga_9$) $R_{0.67}M$ (R_4M_6) and *MTM* ($M_6T_6M_6$) slabs alternate in the ratio 1:1. In the $Sc_{0.67}Fe_2Si_5$-type structure consecutive $R_{0.67}M$ layers are separated by two *MTM* slabs. In the

structure of $R_{0.67}Ni_2Al_6$ ($ErNi_3Al_9$) there is an additional *M* (M_3) layer between consecutive *MTM* ($M_3T_3M_3$) slabs, whereas in the structure of $Gd_{1.33}Pt_3Al_8$ ($Er_4Pt_9Al_{24}$) each $R_{0.67}M$ (R_2M_3) slab is situated between a single and a double *MTM* ($M_3T_3M_3$) slab. Structural features of the members of the homologous series $R_{0.67}T_nM_{2n+m}$ are summarized in Table 8.

Conclusions

The Al-rich part of the *R*-*T*-Al systems (*R* – rare-earth metal, *T* – *d*-element of group VIII; > 60 at.% Al) contains a large number of compounds crystallizing with structures that can be decomposed into monoatomic layers with triangular (or derived) mesh.
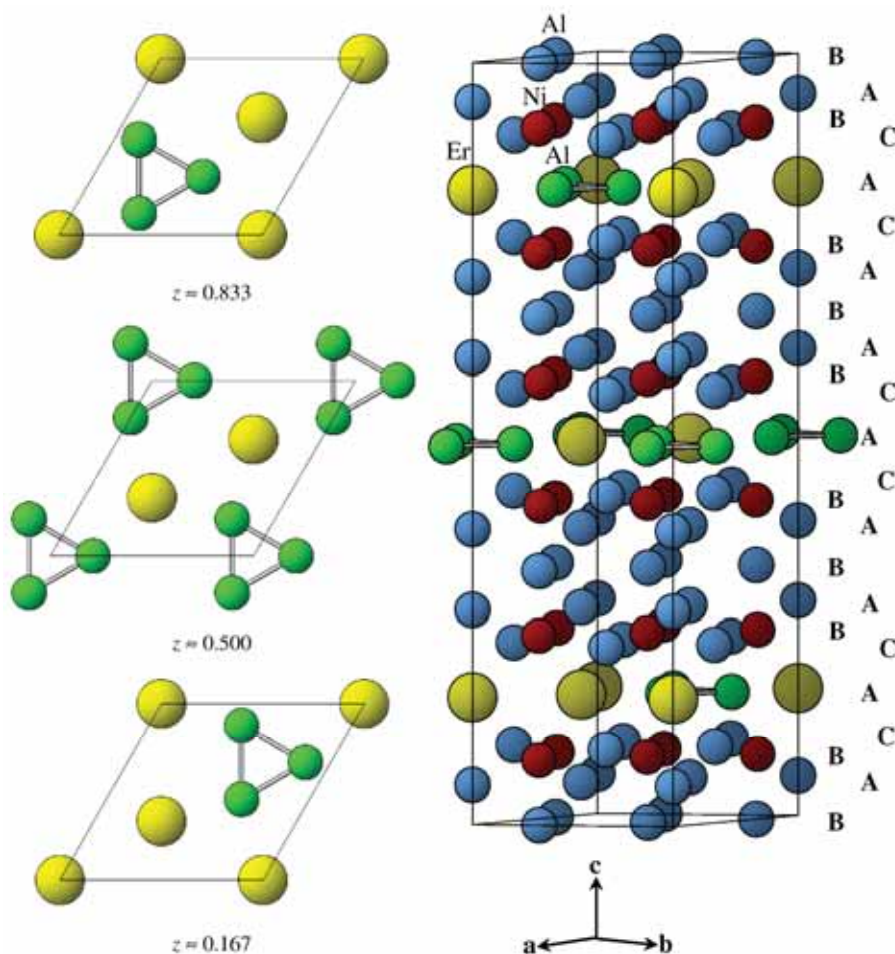
Fig. 12 Stacking of monoatomic layers along [001] and R_2M_3 layers in the $ErNi_3Al_9$ structure.

Three kinds of layer are observed, among which the $R_{0.67}Al$ layer, which can be derived from a close-packed R-atom layer by a disordered or ordered replacement of one-third of the R atoms by Al_3 triangles. Probably, in the real structures the layers are ordered and the observed disorder is being due to stacking faults. Simple stacking rules could be derived, which may help to predict new structures.

References

[1] P. Villars, K. Cenzual (Eds.), *Pearson's Crystal Data, Crystal Structure Database for Inorganic Compounds*, ASM International, Materials Park (OH), 2007.

[2] S. Niemann, W. Jeitschko, *Z. Kristallogr.* 210 (1995) 338-341.

[3] S. Niemann, W. Jeitschko, *J. Alloys Compd.* 221 (1995) 235-239.

[4] J. Niermann., W. Jeitschko, *Inorg. Chem.* 43 (2004) 3264-3270.

[5] B. Fehrmann, W. Jeitschko, *J. Alloys Compd.* 298 (2000) 153-159.

[6] A.I. Tursina, S.N. Nesterenko, E.V. Murashova, I.V. Chernyshev, H. Noël, Yu.D. Seropegin, *Acta Crystallogr. E* 60 (2004) i145-i146.

[7] Yu.Ya. Lutsyshyn, Ya.O. Tokaychuk, R.E. Gladyshevskii, R. Černý, Ya.M. Kalychak, *Ukr. Khim. Zh.*, in press.

[8] K. Turban, H. Schäfer, *J. Less-Common Met.* 40 (1975) 91-96.

[9] Ya.P. Yarmolyuk, R.M. Rykhal', O.S. Zarechnyuk, *Tez. Dokl. II Vses. Konf. Kristallokhim. Intermet. Soeden.* (1974) 39-40.

[10] A.I. Tursina, N.G. Bukhan'ko, A.V. Gribanov, H. Noël, T. Roisnel, Yu.D. Seropegin, *J. Alloys Compd.* 400 (2005) 194-196.

[11] R.E. Gladyshevskii, K. Cenzual, E. Parthé, *J. Solid State Chem.* 100 (1992) 9-15.

[12] O. Tougait, J. Stepien Damm, V.I. Zaremba, H. Noël, R. Troc, *J. Solid State Chem.* 174 (2003) 152-158.

[13] D. Gout, T.J. Barker, O. Gourdon, *Chem. Mater.* 17 (2005) 3661-3667.

[14] R.E. Gladyshevskii, E. Parthé, *Acta Crystallogr. C* 48 (1992) 232-236.

[15] G. Cordier, C. Dietrich, T. Friedrich, *Z. Kristallogr.* 211 (1996) 627-628.

[16] R.E. Gladyshevskii, K. Cenzual, H.D. Flack, E. Parthé, *Acta Crystallogr. B* 49 (1993) 468-474.

[17] R.M. Rykhal', O.S. Zarechnyuk, Ya.P. Yarmolyuk, *Sov. Phys. Crystallogr.* 17 (1972) 453-455.

[18] R.M. Rykhal', O.S. Zarechnyuk, Ya.P. Yarmolyuk, *Dopov. Akad. Nauk Ukr. RSR, Ser. A* (1977) 265.

[19] B.Ya. Kotur, M. Bruvo, *Sov. Phys. Crystallogr.* 36 (1991) 787-789.

[20] S.E. Latturner, M.G. Kanatzidis, *Inorg. Chem.* 41 (2002) 5479-5486.

[21] V.M.T. Thiede, B. Fehrmann, W. Jeitschko, *Z. Anorg. Allg. Chem.* (625 1999) 1417-1425.

[22] Yu. Grin, R.E. Gladyshevskii, O.M. Sichevich, V.E. Zavodnik, Ya.P. Yarmolyuk, I.V. Rozhdestvenskaya, *Sov. Phys. Crystallogr.* 29 (1984) 528-530.

[23] J. Niermann, B. Fehrmann, M.W. Wolff, W. Jeitschko, *J. Solid State Chem.* 177 (2004) 2600-2609.

[24] R.E. Gladyshevskii, O.R. Strusievicz, K. Cenzual, E. Parthé, *Acta Crystallogr. B* 49 (1993) 474-478.

[25] Ya.P. Yarmolyuk, R.M. Rykhal', L.G. Akselrud, O.S. Zarechnyuk, *Dopov. Akad. Nauk Ukr. RSR, Ser. A* (9) (1981) 86-90.

[26] O.S. Zarechnyuk, P.I. Krypyakevych, *Sov. Phys. Crystallogr.* 7 (1962) 436-446.

[27] T. Hahn (Ed.). *International Tables for Crystallography*, *Vol. A,* Kluwer, Dordrecht, The Netherlands, 2002, 911 p.

[28] G.M. Sheldrick. *SHELX-97 – WinGX Version. Release 97-2,* University of Göttingen, Germany, 1997.

[29] E. Parthé, L. Gelato, B. Chabot, M. Penzo, K. Cenzual, R. Gladyshevskii, *TYPIX - Standardized Data and Crystal Chemical Characterization of Inorganic Structure Types*, Springer-Verlag, Berlin, Germany, 1993/1994, Vols. 1-4, 1596 p.